Identification of system misregistrations during AO-corrected observations

Clémentine Béchet[1a], Johann Kolb[2], Pierre-Yves Madec[2], Michel Tallon[1], and Éric Thiébaut[1]

[1] Université de Lyon, F-69000 Lyon, France Centre de Recherche Astrophysique de Lyon
[2] European Southern Observatory, Karl-Schwarzschild Str. 2, 85 748 Garching b. Muenchen, Germany

Abstract. The adaptive optics facility (AOF) designed for the Very Large Telescope (VLT) in Chile will be equipped with a deformable secondary mirror (DSM). The calibration procedure of the interaction matrix, which characterizes the system and the relationship between the DSM commands and the wavefront sensors (WFS) slopes, will be more complex than for the previous systems at the VLT since it will have to be measured on sky and for a much larger number of degrees of freedom (1170 actuators). In addition, gravity or temperature variations for instance are likely to introduce slow evolution of the matching between the DSM and the WFS geometry. This can occur during observations and therefore degrade the adaptive optics (AO) correction. To relax the need of frequent painful calibrations and to prevent a loss of performance due to misregistrations, we investigate how to track the evolution of the interaction matrix errors in closed-loop without introducing any degradation in the observations. This is done thanks to identification methods and optimization theory. First, we formally describe the closed-loop problem and its specificities. Then, we present a solution, based on the optimization of the error of estimates of the WFS slopes, at the output of the closed-loop AO. The performance of this method and its limitations are analyzed formally and thanks to numerical simulations of an AO system somehow characteristic of the ones expected in the AOF.

1 Introduction

In 2014, one of the VLT (*Very Large Telescope*) 8-meter telescopes will be equipped with the adaptive optics facility (AOF) [1], which consists of replacing the conventional secondary mirror by a deformable secondary mirror (DSM) and integrating a 4-LGS (laser guide star) unit behind this DSM. This major change will transform the unit into the first adaptive telescope at Cerro Paranal (Chile). The strategy for AOF today is to model the system with a pseudo-synthetic interaction matrix (IM) [2] and to build the control matrix (CM) from it. The IM will be computed from a global theoretical model of the AOF (synthetic) with a restricted number of parameters calibrated during the characterization phase of the AOF (*e.g.* the actuators influence functions of the DSM) or later on-sky. This limited number of parameters is much smaller than the number of elements in the IM and they usually have a physical meaning (*e.g.* shifts/rotation angle of the DSM with respect to the sensors axis, pixel scale, centroiding gain).

In adaptive telescopes, the changes of the adaptive optics (AO) system during observations, induced for instance by gravity or temperature variations, are expected to be more important since the AO components are no longer gathered in an optical bench isolated from the main telescope movements. In addition, the VLT design without intermediate focus will prevent calibrating the interaction IM using an internal reference source. To relax the need of frequent on-sky calibrations and to prevent a loss of performance due to appearing misregistrations, we search for a method to track the evolution of the IM parameters in closed-loop without introducing any degradation of the observations.

To answer this, the paper presents a method for the identification of the parameters of the IM and its associated control matrix (CM) during closed-loop on sky. The outline of this paper is as follows. Section 2 defines the context of this study and highlights the sensitivity of an AO system to parameters changes and the need for an identification method for IM/CM parameters. In Section 3, a method is presented with the criterion used for the estimation of the parameters. In Sect. 4, the benefits of the method are demonstrated thanks to first numerical simulations.

[a] Clementine.Bechet@univ-lyon1.fr

2 Context : Sensitivity to misregistrations

Some parameters of the IM and CM of the AOF will be calibrated in laboratory tests and their value may never change with time, while others may need more regular calibration and may be subject to (slow) evolution with time and observing conditions. Calibration of these parameters is expected before observation. If these parameters happen to become different during the AO-corrected observation, *i.e.* if misregistrations appear, the performance will be degraded. All through this paper, we name misregistrations the discrepancies between registered parameters values and the true values of the system. In that sense, the reference, *i.e.* no misregistration, does not mean that the DSM and the WFS are aligned in a particular way (Fried geometry for instance), but that the registered values of alignment are the true ones. It is out of the scope of this paper to do a complete sensitivity study for AOF, but some examples are provided since this constitutes a direct driver for the requirements on on-sky closed-loop parameters identification method developed below.

2.1 Impact of a shift misregistration in end-to-end simulations of AOF

The AOF will be used for GALACSI and GRAAL AO systems. GALACSI presents 2 possible modes of AO correction: laser tomography AO (LTAO, narrow-field mode) or ground layer AO (GLAO, wide-field mode). The performance analysis of GALACSI shows, thanks to end-to-end simulations [3], how a shift misregistration between the DSM and the WFS axes degrades the correction in Fig. 1. The left graph shows that the Strehl ratio significantly drops down for LTAO when shifts misregistrations exceed 20% of the subaperture size. On the right, the benefit of the GLAO correction is expressed as the gain in Ensquared Energy compared to no AO correction. In this mode, a shift of 20% of subaperture size is a limit to ensure the required performance, *i.e.* higher gain than 1.5.

A different approach has been followed in GRAAL physical analysis report [4] to setup the final accuracy required to 0.7% of the 8m-pupil including all error terms. Thus, for this GLAO system, a reasonable target could be 0.5%, which translates into 20% of a subaperture size, again.

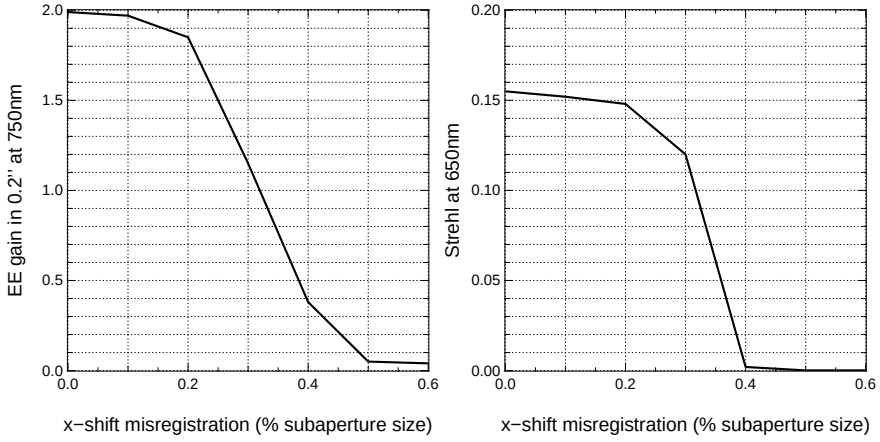

Fig. 1. AO correction performance *vs* shift misregistration (displacement) estimated from end-to-end simulations of GALACSI [3]. Left: Strehl ratio for the LTAO correction. Right: gain in Ensquared Energy in a $0.2" \times 0.2"$ box for the GLAO correction.

2.2 Impact of shifts and rotation misregistrations in a simplified AOF-size simulation

The current identification study required building a dedicated simplified AO simulator, able to accurately model the effects of geometrical parameters variations, avoiding artefacts potentially spoiling the analysis. The simplified simulations presented in this paper are thus characterized by:

- a square telescope aperture of 8 meters
- an infinite size deformable mirror (DM) shell (to avoid particular edge effects in a first step)
- 40×40 actuators on the DM, with 30% cross coupling and polynomial influence functions [6]
- a single Shack-Hartmann wavefront sensor (WFS) of 40×40 subapertures (geometrical model)
- a single natural guide star
- a $\tau-$frame delay closed-loop correction ($\tau = 2$)
- an integrator for the control law

This configuration, different from the real DSM of the AOF, constitutes a more conventional context of preliminary demonstration of on-sky closed-loop identification and update of parameters. The sensitivity of the AO correction to both shifts and rotation misregistrations is illustrated in Fig. 2. On the left, the AO performance is degraded (in terms of average wavefront error - WFE - in nm rms over the 8-m aperture during 14 000 loops) when the amplitude of the misregistration increases.

The photon noise is simulated in the system, with a standard deviation σ_{noise} expressed in nm rms between 2 sides of a subaperture, following

$$\sigma_{\text{noise}} \simeq \sqrt{\frac{\text{FWHM}^2\, d_l^2}{8\, \ln 2\, N_{\text{ph}}}}, \tag{1}$$

where FWHM is the full width at half maximum of the spot in the subaperture (rad.), d_l is the subaperture size (m) and N_{ph} is the average number of detected photons per subaperture per frame. Various noise levels σ_{noise} are simulated (various symbols) in Fig. 2. The fitting error is close to 50nm rms which, together with the 2 ms correction delay, makes the performance never better than 50 nm rms even at low noise level.

The misregistration amplitude (shifts and rotation) is characterized here by

$$||\delta p|| = \sqrt{\delta x^2 + \delta y^2 + tan(\delta\theta)^2\, R_{\text{rot}}^2} \tag{2}$$

where δx and δy are the 2D-shift misregistrations, $\delta\theta$ is the rotation misregistration (radians) and R_{rot} is a characteristic radius value in order to obtain homogeneous dimensions in the evaluation of the parameter misregistration δp amplitude. The value of R_{rot} has been chosen equal to 1.8 m in order to minimize the dispersion of the curves on the left of Fig. 2 for every noise level. The simulated AO appears less sensitive to shift misregistrations (up to $||\delta p|| < 30\%$) than in the full AOF from Fig. 1.

Instabilities are observed beyond $||\delta p|| \sim 35\%$ of subaperture size almost independently of the noise level. This particular behaviour comes from the fact that the same integrator gain, same IM and same CM have been used for all noise conditions. Another way (less concise) to represent such results is shown on the right of Fig. 2. At location $(0, 0)$, there is no shift misregistration, and the closed-loop is stable (filled circles) up to a differential rotation of 0.86 degree (1.15 degree is the largest circle, equivalent to a shift of 15% subaperture size at $R_{\text{rot}} = 1.8$ m). At location $(0.2, 0.2)$, the closed-loop is stable only if there is no rotation misregistration (small filled circle). There instability seems to be triggered by the value of $|\delta x| + |\delta y|$ more than by $||\delta p||$ from Eq. (2). This highlights that no perfect characterization of the misregistration amplitude $||\delta p||$ including shifts and rotation has been found so far. This problem was expected because the rotation locally acts as a shift, but globally has a more complex effect, impacting on both $x-$ and $y-$alignments. It is beyond the scope of this paper to deeply study this. The aim of Figs. 1 and 2 is:

- to present for once a global study of shifts and rotation misregistrations at the same time;
- to show that the performance is very weakly affected by misregistrations below 15-20% of the subaperture size;
- to show the stability range for such misregistrations.

The second point is important since one can then wonder if effects inside that range could be detected and estimated with accuracy by the identification method we investigate.

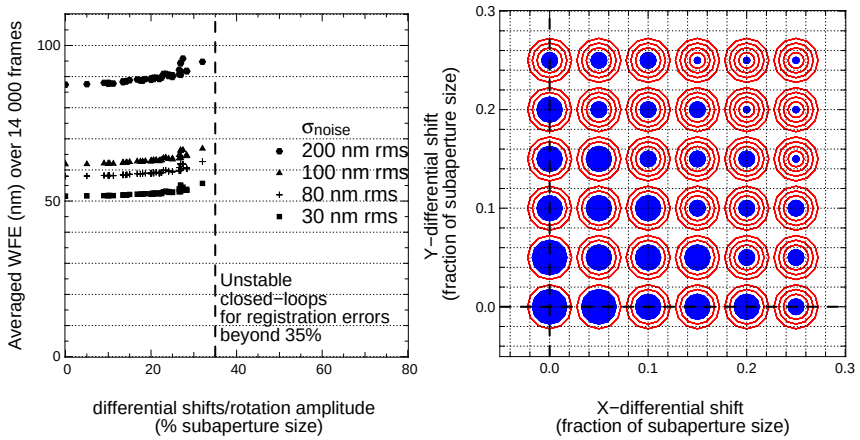

Fig. 2. AO sensitivity to shifts and rotation misregistrations. Left: Average wavefront error (nm rms) over the 8-m square aperture during the 14 000 last loops *vs* $\|\delta p\|$ defined in Eq. (2). Right: representation of stable (filled circles) and instable (circles) closed-loop as a function of the shifts misregistrations ($x-$ and $y-$axis) and the rotation angle misregistration (circle radii for increasing rotations in degree: 0, 0.29, 0.57, 0.86, 1.15) for a noise level of 80 nm rms.

2.3 Constraints and main goals

The results of Sects. 2.1 and 2.2 drive us towards the requirement of an identification method to estimate the misregistrations parameters during the closed-loop on-sky AO correction directly from the sequence of the WFS slopes and commands (telemetry of the AO system). According to the sensitivity analysis above, our requirement is to reach an estimation accuracy better than 10% of subaperture size in order to avoid AO performance degradation. In addition, the major and original challenge in the identification study presented here is that no additional disturbance is introduced in the AO loop. This is to prevent any harmful impact on astrophysical data, to fully exploit the available AO data (telemetry) and to avoid complexifying the system with an additional signal and detection process.

Such identification of parameters is expected to be done online, but at a lower frequency (maybe every minute) than the closed-loop correction, since the parameters are assumed to evolve slowly (on the scale of several minutes). When non-zero misregistrations are estimated, the baseline of the AOF is not to realign the DSM, but to update the IM and CM parameters numerically instead, in order to adapt the reconstruction and control computations in the real-time computer (RTC). Last but not least, the CM is not planned to be regularly updated, but only in the case the misregistration exceeds a given threshold probably close to 10% of subaperture size. This constraints comes from the fact that the RTC of the AOF, SPARTA [5], may need to skip up to 40 loops to load a new CM, thus risking a degradation of the AO correction.

3 Criterion for parameters identification

Identification of system parameters in closed-loop is not an easy problem to solve in theory [7,8] if one does not apply additional known disturbance to probe the system. Typical synchronized detection methods can not be applied if no specific and periodic command is added to the deformable mirror commands. The only available command set is recorded in the telemetry and is constrained by the fact that the AO system permanently tries to compensate for the atmospheric turbulence. In this section, the AO equations and notations are described, and the identification method is detailed.

3.1 Adaptive optics equations

The AO system is characterized by the following closed-loop equations. At every discrete time k,

$$\boldsymbol{d}_k = S(w_k) - \mathbf{G}(\boldsymbol{p}) \cdot \boldsymbol{a}_k + \boldsymbol{e}_k \quad \forall k \geq 0\,, \tag{3}$$

where $\mathbf{G}(\boldsymbol{p})$ is the IM associated to its parameters $\boldsymbol{p}$, S is the linear model of relationship between the turbulent atmosphere w_k and WFS data vector $\boldsymbol{d}$, $\boldsymbol{a}$ is the command vector applied to the DM and $\boldsymbol{e}$ is the photon noise vector affecting measurement $\boldsymbol{d}$. Index k, for time step, is used to index all the elements involved in the production of the $k-$th measurement vector. This (arbitrary) index writing is not usual in AO, but it has been chosen here because it provides clearer notations for the identification study. The correction delay then only appears in the control law equation

$$\boldsymbol{a}_k = \begin{cases} 0 & \text{if} \quad 0 \leq k \leq \tau \\ \alpha \boldsymbol{a}_{k-1} + \beta \boldsymbol{a}_{k-2} + \gamma \mathbf{C}(p) \cdot \boldsymbol{d}_{k-\tau} & \text{if} \quad \tau \leq k\,, \end{cases} \tag{4}$$

where α, β and γ are scalars and $\mathbf{C}(p)$ is the CM associated to the registered system and used for the closed-loop correction. Such control law (4) corresponds to the constraints imposed by the AOF RTC [5].

The measurement equation (3) can also be written

$$\boldsymbol{d}_k = -\mathbf{G}(p) \cdot \boldsymbol{a}_k + \boldsymbol{z}_k\,, \quad \text{with} \quad \boldsymbol{z}_k = S(w_k) + \boldsymbol{e}_k\,, \tag{5}$$

where $\boldsymbol{z}_k$ is considered as a disturbance vector, including both turbulence contribution and photon noise, $\boldsymbol{e}_k$. From this new point of view, in Eq. (5), the data $\boldsymbol{d}_k$ are considered to be noisy measurements of the slopes induced by the command vector $\boldsymbol{a}_k$. This disturbance $\boldsymbol{z}_k$ follows zero-mean Gaussian statistics and its covariance matrix can be written

$$\mathbf{C}_{\mathbf{z_k}} = \left\langle \boldsymbol{z}_k \cdot \boldsymbol{z}_k^{\mathrm{T}} \right\rangle = \left\langle \mathbf{S}(w_k) \cdot \mathbf{S}(w_k)^{\mathrm{T}} \right\rangle + \left\langle \boldsymbol{e}_k \cdot \boldsymbol{e}_k^{\mathrm{T}} \right\rangle = \left\langle \boldsymbol{s}_k \cdot \boldsymbol{s}_k^{\mathrm{T}} \right\rangle + \left\langle \boldsymbol{e}_k \cdot \boldsymbol{e}_k^{\mathrm{T}} \right\rangle = \mathbf{C}_{\mathbf{s_k}} + \mathbf{C}_{\mathbf{e_k}} \tag{6}$$

$$= \mathbf{C}_\mathbf{s} + \mathbf{C}_\mathbf{e} = \mathbf{C}_\mathbf{z}\,, \tag{7}$$

where $\boldsymbol{s}_k$ is the noiseless measurement of the turbulence w_k. Turbulence and noise are considered as stationnary process at the scale of our study, so the covariance matrices of $\boldsymbol{s}_k$ and $\boldsymbol{e}_k$ are independent of k, and written $\mathbf{C}_\mathbf{s}$ and $\mathbf{C}_\mathbf{e}$ respectively in Eq. (7). The identification of the interaction matrix parameters $\boldsymbol{p}$ based on the measurement model in Eq. (5) appears not easy, because of

1. the temporal correlation between $\boldsymbol{d}_k$ at different k;
2. the spatial correlation between elements of $\boldsymbol{d}_k$ from different subapertures and possibly different guide stars, *via* $\mathbf{C}_\mathbf{s}$;
3. the spatial and temporal correlations between the disturbance $\boldsymbol{z}_k$ and the commands $\boldsymbol{a}_k$.

Instead of using Eq (5), we can also use the difference between two successive data vectors [9]

$$\delta \boldsymbol{d}_k = \boldsymbol{d}_{k+1} - \boldsymbol{d}_k = -\mathbf{G} \cdot \delta \boldsymbol{a}_k + \delta \boldsymbol{z}_k \quad \text{where} \quad \delta \boldsymbol{a}_k = \boldsymbol{a}_{k+1} - \boldsymbol{a}_k \quad \text{and} \quad \delta \boldsymbol{z}_k = \boldsymbol{z}_{k+1} - \boldsymbol{z}_k\,. \tag{8}$$

The new disturbance $\delta \boldsymbol{z}_k$ follows zero-mean Gaussian statistics of covariance matrix

$$\mathbf{C}_{\delta z} = \left\langle \delta \boldsymbol{z}_k \cdot \delta \boldsymbol{z}_k^{\mathrm{T}} \right\rangle = \left\langle (\boldsymbol{z}_{k+1} - \boldsymbol{z}_k) \cdot (\boldsymbol{z}_{k+1} - \boldsymbol{z}_k)^{\mathrm{T}} \right\rangle \tag{9}$$

$$= \left\langle (\mathbf{S}(\delta w_k) + \delta \boldsymbol{e}_k) \cdot (\mathbf{S}(\delta w_k) + \delta \boldsymbol{e}_k)^{\mathrm{T}} \right\rangle = \left\langle \mathbf{S}(\delta w_k) \cdot \mathbf{S}(\delta w_k)^{\mathrm{T}} \right\rangle + \left\langle \delta \boldsymbol{e}_k \cdot \delta \boldsymbol{e}_k^{\mathrm{T}} \right\rangle \tag{10}$$

$$\tag{11}$$

The idea of such approach is to transform the estimation problem

1. preserving linearity and Gaussian statistics;
2. providing a disturbance covariance matrix $\mathbf{C}_{\delta z}$ which could be better approximated by a diagonal matrix, approximately equal to twice the photon noise covariance matrix $\mathbf{C}_e$;
3. and approximately decorrelating signal ($\mathbf{G} \cdot \delta \boldsymbol{a}_k$) and disturbance ($\delta \boldsymbol{z}_k$).

3.2 Identification method

The identification of the parameters $\boldsymbol{p}$ of matrix $\mathbf{G}(p)$ is based on a sequence of $\boldsymbol{\delta d}_k$ and $\boldsymbol{\delta a}_k$ recorded during closed-loop AO (telemetry). There is no linearity assumption for the relation between the parameters $\boldsymbol{p}$ and the matrix coefficients of $\mathbf{G}(\boldsymbol{p})$. The IM is defined as a parametric model $\mathbf{G}(\boldsymbol{p})$, built from DM influence functions and a Shack-Hartmann linearized model. Using N sets of differential data $\delta\boldsymbol{d}_{k\,\Delta T}$ separated by ΔT frames (ΔT large enough to avoid correlations between the asociated $\delta\boldsymbol{z}_k$ and $\delta\boldsymbol{z}_{k+\Delta T}$), one could fit the interaction matrix parameters $\boldsymbol{p}$ using a maximum likelihood approach and minimizing the criterion

$$\chi^2_{N,\Delta T}(\boldsymbol{p}) \simeq \frac{1}{2}\sum_{k=1}^{k=N}(\delta\boldsymbol{d}_{k\,\Delta T} + \mathbf{G}(\boldsymbol{p})\cdot\delta\boldsymbol{a}_{k\,\Delta T})^{\mathrm{T}}\cdot\mathbf{C}_{\delta z}^{-1}\cdot(\delta\boldsymbol{d}_{k\,\Delta T} + \mathbf{G}(\boldsymbol{p})\cdot\delta\boldsymbol{a}_{k\,\Delta T}) \tag{12}$$

The criterion in Eq. (12) is computed in practice assuming $\mathbf{C}_{\delta z} \simeq 2\,\mathbf{C}_e$. The validity of this approximation is the subject of a current theoretical study, but it is already used in this paper based on results we observed in numerical simulations. A non-linear optimization algorithm, which is a Levenberg-Marquardt algorithm modified to take into account a *trust region*, is used to minimize this criterion [10].

The estimation method does not rely on any assumption about the AO control law Eq. (4), but its accuracy is expected to depend on it since the control law influences the sequence of recorded commands. The theoretical accuracy issue is also under study.

When considering LGS WF sensing and partial tip-tilt correction on the related measurements, the residuals $(\delta\boldsymbol{d}_{k\,\Delta T} + \mathbf{G}\cdot\delta\boldsymbol{a}_{k\,\Delta T})$ in the criterion are computed after removal of the tip-tilt contribution. In GLAO and LTAO configurations, the correlation between the signal $(\mathbf{G}\cdot\delta\boldsymbol{a}_{k\,\Delta T})$ and the noise (turbulence and photon noise) is expected to be minor compared to a single-conjugate AO. An improvement of the method accuracy is thus expectable, although no quantified gain is demonstrated so far.

4 First numerical results on AOF-size simulated system

In the end-to-end simulations of the "square aperture" single-conjugate AO system, we use a 4-layer atmosphere, shifted with constant wind (equivalent to ~ 10 m.s^{-1}) in various (although constant) directions during 15 seconds (*i.e.* 15 000 loops at 1 kHz). The same atmosphere is used for all the simulations. For the AOF, the spot size on the Shack-Hartmann in the non-elongated direction, is expected to be ~ 1 to 1.3 arcseconds with about $N_{\mathrm{ph}} = 40$ photodetections per frame per subaperture. This leads to $\sigma_{\mathrm{noise}} \simeq 65-85$ nm rms (see Eq. (1)). The wavefront sensing is simulated with a geometrical model. The only misregistrations here are $(x, y)-$shifts and rotations of the DM.

Simulations start with IM and CM built from registered parameters p^{reg}, and possibly different from the true parameters $p^{\mathrm{true}} = p^{\mathrm{reg}} + \delta p$. Every 3 000 loops, a two-step process is applied:

1. Identification of parameters, minimizing of $\chi^2_{N,\Delta T}(\boldsymbol{p})$.
2. IM/CM registered parameters are numerically updated if the misregistration exceeds a threshold.

The identification relies on the sequence of the 2 000 last recorded data and commands with $\Delta T = 23$ frames and $N = 130$. The residuals do not include information from subapertures on the edges, and only 2 iterations of the iterative Levenberg-Marquardt algorithm are proceeded. The update of the CM (and its parameters) is applied only if the global misregistration $\|\delta p\| = \|p^{\mathrm{true}} - p^{\mathrm{reg}}\|$ exceeds a given threshold. Here a threshold of 10% of a subaperture size was chosen, being a reasonable limit to prevent instabilities (see Sect. 2).

In Fig. 3, a simulation with high photon noise level in the AO system ($\sigma_{\mathrm{noise}} = 200$ nm rms) shows how the identification method allows to converge towards the true parameters. On the left, the registered values of shifts and rotation at time 0 are represented with big white markers. Every 3 seconds, the two-step process (identification and possible update) is applied (CM parameters = big filled markers). On the right, the residual wavefront averaged over the pupil and over time (WF error in nm rms) is represented, showing the difference between a closed-loop without CM parameters update

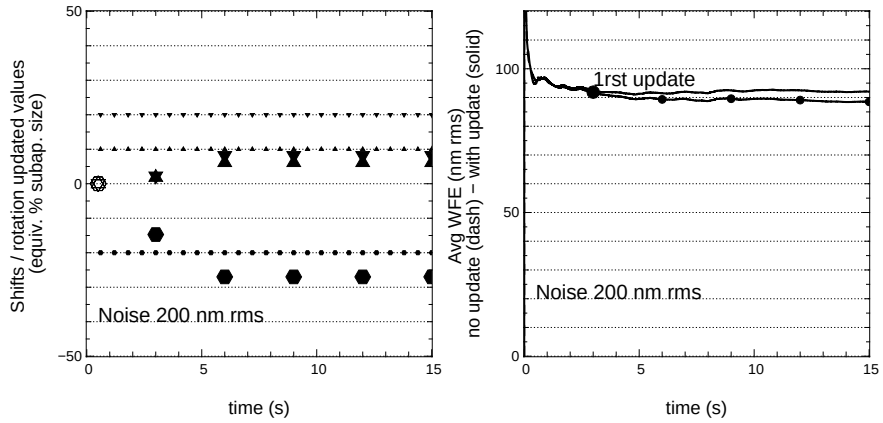

Fig. 3. Identification and update of CM parameters during closed-loop simulation (15 000 loops) of a high noise level AO (σ_{noise} = 200 nm rms). On the left: Triangles : $x-$shift. Inverted triangles: $y-$shift. Hexagons: rotation angle, $tan(\theta)\, R_{\text{rot}}$. Horizontal lines of small markers: true parameters. Large white markers at time 0: registered parameters when starting the closed-loop. On the right: evolution of the average residual WF over the aperture and over time. Dash/Above: without update of CM parameters. Solid/Below: with update of CM parameters.

(dash) and the same closed-loop with CM parameters update (solid). The convergence of the identification method allows the system to overcome medium misregistrations. The significant discrepancies between true and updated parameters on the left of Fig. 3 are due to the update threshold (here 10% of a subaperture size). Here the identification only slightly benefits the AO correction in terms of WFE (right of Fig. 3) because the dominating error in the system remains (photon noise).

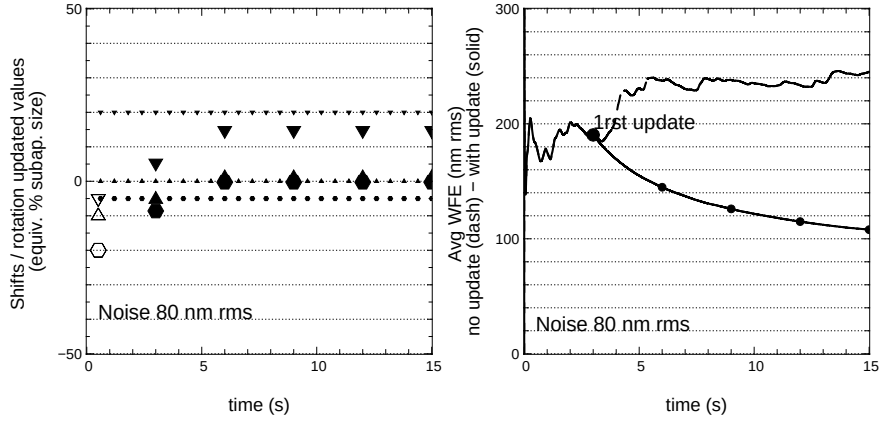

Fig. 4. Same as Fig. 3 but for a typical AO noise for the AOF, *i.e.* σ_{noise} = 80 nm rms.

Next, with a more typical noise level for the AOF (σ_{noise} = 80 nm rms) in Fig. 4, the results are more impressive. Very large misregistrations were applied at the beginning of the simulation and implied an integrator gain of 0.1 to manage to close the loop. On the right part of Fig. 4, the stabilization of the AO correction is observed (solid), as opposed to an instable behaviour if no parameters identification is applied. Identification here leads to a highly improved AO correction.

The identification method was also demonstrated to work with LGS if the tip-tilt contribution to the residuals is not taken into account for the criterion computation. The impact of an error on the AO correction delay assumption was also investigated. Simulating an AO system with a 2-frame delay in Fig. 5, we tried to apply identification and update assuming a wrong delay value (τ = 1 frame on the

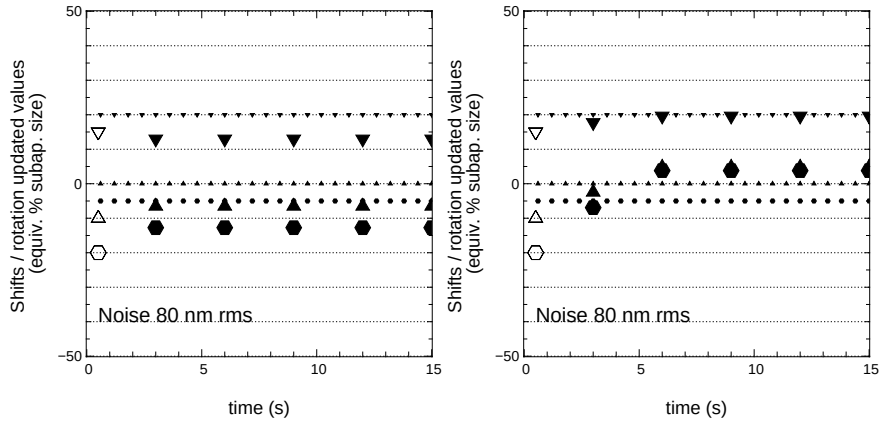

Fig. 5. Same as legend as on the left of Fig. 4, but the identification method is computed with a wrong value for the AO delay (Left: 1 frame - Right: 3 frames). True delay (simulated) is 2 frames.

left, $\tau = 3$ frame on the right). The identification still manages to keep track of the true parameters with a better accuracy than 10% of a subaperture size in the case of an overestimated delay (3 frames). Errors are slightly larger for an understimated delay (1 frame).

5 On-going and future work

As a conclusion, this paper presents an identification method for misregistration parameters during closed-loop AO-corrected observations. In preliminary simulations, the method matches the goals driven by the AOF requirements, with an accuracy better than 10% of a subaperture size, and a numerical update of the command matrix when misregistrations exceed a threshold. The original assets of the method lie in the fact that no additional disturbance is introduced in the AO system. It exploits the AO telemetry minimizing a global criterion and it is computationnally reasonable. It can handle undetermined modes (*e.g.* tip-tilt) and it is robust to AO correction delay uncertainty.

The principle and efficiency of the identification method being validated on a simplified AO system, the behaviour of the method for a more realistic model of the AOF system is now under investigation. In parallel to these simulation advances, a theoretical analysis of the method is currently studied in order to be able to predict the expectable identification accuracy depending on atmospheric conditions, noise level, control parameters and fitting parameters (*e.g.* ΔT, N and number of iterations). Finally, the issue of multi-LGS configuration needs to be tackled to completely answer the AOF problem and to pave the way to all the ELT AO systems with multiple guide stars.

References

1. R. Arsenault, *et al.*, Proc. of SPIE Conference, **7736**, (2010) 77360L
2. J. Kolb, ESO Technical Report, VLT-TRE-ESO-22200-5114 (2011)
3. M. Le Louarn, ESO Technical Report, VLT-TRE-ESO-14675-4483 (2009)
4. J. Paufique, ESO Technical Report, VLT-TRE-ESO-14850-4196 (2009)
5. P.-Y. Madec, ESO Technical Report, VLT-SPE-ESO-22000-4723 (2009)
6. M. Le Louarn, Compte Rendus Physique, **6**, (2005) 1070-1080.
7. L. Ljung, *System identification - Theory for the user*, 2^{nd} Edition, (PTR Prentice Hall, Upper Saddle River, N.J., 1999)
8. A. Chiuso, R. Muradore and E. Marchetti, Proc. of CDC., (2008) 750-755
9. H. Bonnet, ESO Technical Report, E-TRE-ESO-131-0394 (2009)
10. I. Tallon-Bosc, *et al.*, Proc. of SPIE Conference, **7013**, (2008) 70131J